Modelling galaxy merger time-scales and tidal destruction

Vimal Simha[1,2,3,4]⋆ and Shaun Cole[4]

[1]*University of the Western Cape, Bellville, Cape Town 7535, South Africa*
[2]*South African Astronomical Observatories, Observatory, Cape Town 7925, South Africa*
[3]*African Institute for Mathematical Sciences, Muizenberg, Cape Town 7945, South Africa*
[4]*Institute for Computational Cosmology, Department of Physics, Durham University, South Road, Durham DH1 3LE, UK*

ABSTRACT

We present a model for the dynamical evolution of subhaloes based on an approach combining numerical and analytical methods. Our method is based on tracking subhaloes in an *N*-body simulation up to the latest epoch that it can be resolved, and applying an analytic prescription for its merger time-scale that takes dynamical friction and tidal disruption into account. When applied to cosmological *N*-body simulations with mass resolutions that differ by two orders of magnitude, the technique produces halo occupation distributions that agree to within 3 per cent. This model has now been implemented in the GALFORM semi-analytic model of galaxy formation.

Key words: galaxies: general – galaxies: groups: general – galaxies: haloes – galaxies: interactions.

1 INTRODUCTION

The evolution of the Universe in the standard Λ cold dark matter (ΛCDM) cosmological model is characterized by hierarchical structure formation where small haloes form first, and subsequently merge to form larger haloes. High resolution *N*-body simulations have indicated that massive haloes retain a substantial amount of substructure (Klypin et al. 1999; Moore et al. 1999; Springel et al. 2001), consisting of bound dark matter clumps orbiting within the potential of their host halo. Evidently, such subhaloes were themselves independent, self-contained haloes in the past, before merging with a more massive halo. If sufficiently massive, these subhaloes were sites of baryon dissipation and star formation in the past. There are many indications, from studies of the statistical properties of how galaxies and substructures populate haloes, that galaxies in groups and clusters are in fact the observational counterparts of subhaloes. For example, Colín et al. (1999) and Kravtsov et al. (2004) show that the autocorrelation functions of substructures in high-resolution *N*-body simulations are in good agreement with the observed autocorrelation functions of galaxies. On the theory side, Kravtsov et al. (2004) find that the distribution of subhaloes in high-resolution *N*-body simulations is similar to that of smoothed particle hydrodynamics (SPH) galaxies in Berlind et al. (2003) and Zheng et al. (2005), and Simha et al. (2012) find good agreement between the properties of galaxies in their SPH simulation and the properties of haloes in their matched *N*-body simulation.

Using *N*-body simulations to study galaxy formation requires a framework for populating dark matter haloes with galaxies. One approach is to employ semi-analytic models that use analytic techniques and phenomenological recipes to follow the evolution of baryons within dark matter haloes. An alternative is to eschew assumptions about baryonic physics and use an empirical approach to relate observed galaxy properties to dark matter halo properties. One popular approach in this class of models is abundance matching, which assumes a monotonic relationship between galaxy luminosity and halo mass. Alternatively, galaxy formation can be studied using hydrodynamic simulations that model gas physics and incorporate gas cooling, star formation and feedback. However, hydrodynamic cosmological simulations are computationally expensive, and as a result, typically employ smaller box sizes than pure *N*-body simulations.

A key aspect of studying galaxy formation within the CDM paradigm is to understand the fate of galaxies following halo mergers – how and when galaxy mergers happen, how and when galaxies are tidally disrupted and what ultimately happens to galaxies that fall in to more massive haloes. In this paper, we model the dynamical evolution of subhaloes and their galaxies using a combination of numerical and analytical methods.

The formation of dark matter haloes through the growth of dark matter perturbations can be studied numerically using dissipationless cosmological simulations. But haloes do not evolve in isolation from each other. When a halo enters the virial radius of a more massive halo, its evolution becomes more complex than that of an independent halo. After falling in to a more massive halo, (sub)haloes experience tidal forces that cause mass-loss, and even complete disruption under extreme circumstances.

⋆ E-mail: vimalsimha@gmail.com

Furthermore, satellite subhaloes orbiting within a host halo lose energy and angular momentum through dynamical friction, which causes their orbits to sink towards the halo centre.

Galaxy formation models use two principal approaches to model the dynamical evolution of subhaloes and satellite galaxies. The first is to use analytically calculated or physically motivated empirical formulae for various aspects of the dynamical evolution of subhaloes such as the time-scale for merging through dynamical friction, tidal stripping, tidal destruction, etc. (e.g. Lacey & Cole 1993; Boylan-Kolchin, Ma & Quataert 2008; Jiang et al. 2008). An alternative approach, that avoids simplifying assumptions, is to use an *N*-body simulation to follow the dynamic evolution of subhaloes. *N*-body simulations capture the complexity of the physics of tidal disruption and dynamical friction, and do not require simplifying assumptions, either about the physical processes or about the distribution of orbital parameters. However, subhalo merging and disruption are affected by finite force and mass resolution. Insufficiently resolved subhaloes disrupt artificially and on shorter time-scales than well resolved haloes (Klypin et al. 1999). Using a fixed subhalo mass resolution limit, regardless of infall mass, leads to lower mass subhaloes being artificially disrupted more quickly. Furthermore, sufficiently high resolution is required to reproduce dynamical friction.

In subhalo abundance matching (SHAM) models, which assume a monotonic relationship between subhalo mass at infall and galaxy luminosity, it is assumed that each galaxy survives as long as its subhalo can be identified in an *N*-body simulation above a fixed resolution threshold. Some models allow galaxies to survive for a period of time after the disruption of their host subhaloes (Saro et al. 2008; Moster et al. 2010), while, in contrast, Stewart et al. (2009) allow satellite galaxies to be disrupted even when their subhaloes still exist.

In contrast, the GALFORM semi-analytic model uses an analytical formula to calculate the merger time-scale for a satellite galaxy (Cole et al. 2000). Following a halo merger, it is assumed that the galaxy hosted by the less massive halo enters the host halo on an orbit with orbital parameters randomly drawn from a distribution. The merger time-scale is then computed using the analytical formulae of Lacey & Cole (1993) in the GALFORM model of Gonzalez-Perez et al. (2014) and the analytical formulae of Jiang et al. (2008) in the GALFORM model of Lacey et al. (2016). Once this time has elapsed, the galaxy hosted by this subhalo is considered to have merged with the central galaxy of the more massive host halo.

In this paper, we employ a hybrid approach to follow the dynamical evolution of subhaloes. We follow subhaloes in an *N*-body simulation until the point when they can no longer be resolved. We then calculate a merger time-scale using its orbital parameters and mass at the epoch that it was last resolved in the *N*-body simulation. Our formula to calculate the merger time-scale is based on Lacey & Cole (1993), with parameters suitably modified to match our *N*-body simulation results. Our scheme is faithful to the underlying *N*-body simulation, minimizing the reliance on analytically determined orbits. Instead of making assumptions about the orbital parameters of satellites, we track the positions of their associated subhaloes.

Our goal is to provide a simple model for the dynamical evolution of subhaloes that uses the information in an *N*-body simulation, but can produce results that are not affected by numerical artefacts, such as artificial disruption of subhaloes, due to limited resolution. While our model is primarily intended for application in semi-analytic models, it can also be used in other models of galaxy formation that use *N*-body simulations like SHAM models. We assume that once

a subhalo reaches the centre of its host halo, the galaxy associated with the subhalo merges with the central galaxy of the host halo. We also assume that once a subhalo is tidally disrupted, the galaxy it hosts is also tidally disrupted. Therefore, within the context of this paper, subhalo mergers and tidal disruption are synonymous with galaxy mergers and galaxy tidal disruption.

We use two *N*-body simulations, the Millennium Simulation (MS) (Springel et al. 2005) and the higher resolution Millennium II simulation (MS II) (Boylan-Kolchin et al. 2009) to tune our model, constrain its free parameters and demonstrate convergence. We also compare our predicted merger time-scales to those previously used in the GALFORM semi-analytic model. We discuss the physical differences between the two models and discuss the effect this has on studies of galaxy clustering.

In Section 2, we describe our simulation and models for populating our subhaloes with galaxies. In Section 3, we describe our model for dynamical friction and tidal disruption. In Section 4, we discuss our results and the implications of our model on halo occupation distributions (HOD) and galaxy clustering. In Section 5, we summarize our results.

2 SIMULATIONS

We use two simulations, the MS (Springel et al. 2005) and the higher resolution MS II (Boylan-Kolchin et al. 2009). Both simulations follow the evolution of 2160^3 particles from $z = 127$ to 0 in a ΛCDM cosmology (inflationary, cold dark matter with a cosmological constant) with $\Omega_M = 0.25$, $\Omega_\Lambda = 0.75$, $h \equiv H_0/100 \, \text{km} \, \text{s}^{-1} \, \text{Mpc}^{-1} = 0.73$, primordial spectral index $n_s = 1$ and the amplitude of mass fluctuations $\sigma_8 = 0.9$, where σ_8 is the linear theory rms mass fluctuation amplitude in spheres of radius $8 \, h^{-1} \text{Mpc}$ at $z = 0$. These parameter values were chosen to agree with *WMAP* 1-yr data (Spergel et al. 2003), and are different from, but reasonably close to current estimates from the cosmic microwave background (Planck Collaboration XIII 2015). The main difference is that the more recent data favour a lower value of the amplitude of clustering, σ_8. We do not expect small differences in the cosmological parameters to affect our results.

The MS simulates a comoving box that is $500 \, h^{-1} \, \text{Mpc}$ on each side, while the MS II simulates a comoving box that is $100 \, h^{-1} \, \text{Mpc}$ on each side. The simulation particle masses are $m_p = 8.6 \times 10^8 \, h^{-1} \, \text{M}_\odot$ in MS and $6.9 \times 10^6 \, h^{-1} \, \text{M}_\odot$ in MS II.

For each output epoch in each simulation, the friends-of-friends (FOF) algorithm is used to identify groups by linking together particles separated by less than 0.2 times the mean inter particle separation (Davis et al. 1985). The SUBFIND algorithm (Springel et al. 2001) is then applied to each FOF group to split it into a set of self-bound subhaloes. The central subhalo is defined as the most massive subunit of a FOF group. We construct subhalo merger trees that link each subhalo at each epoch to a unique descendent in the following epoch. These merger trees allow us to track the formation history of each (sub)halo that is identified at $z = 0$. Springel et al. (2005) and Boylan-Kolchin et al. (2009) provide a detailed description of these simulations and the post-processing techniques.

2.1 Sham

SHAM is a technique for assigning galaxies to simulated dark matter haloes and subhaloes based on the assumptions that all galaxies reside in identifiable dark matter substructures and that luminosity or stellar mass of a galaxy is monotonically related to the potential

well depth of its host halo or subhalo. Some implementations of SHAM use the maximum of the circular velocity profile as the indicator of potential well depth, while others use halo or subhalo mass. The first clear formulations of SHAM as a systematic method appear in Conroy, Wechsler & Kravtsov (2006) and Vale & Ostriker (2006), but these build on a number of previous studies that either test the underpinnings of SHAM or implicitly assume SHAM-like galaxy assignment (e.g. Colín et al. 1999; Kravtsov et al. 2004; Nagai & Kravtsov 2005).

N-body simulations produce subhaloes that are located within the virial radius of haloes. The present mass of subhaloes is a product of mass build up during the period when the halo evolves in isolation and tidal mass-loss after it enters the virial radius of a more massive halo (e.g. Kazantzidis et al. 2004; Kravtsov et al. 2004). The stellar component, however, is at the bottom of the potential well and more tightly bound making it less likely to be affected by tidal forces. Therefore, several authors (e.g. Conroy et al. 2006; Vale & Ostriker 2006) argue that the properties of the stellar component should be more strongly correlated with the subhalo mass at the epoch of accretion, rather than at $z = 0$.

We assume a monotonic relationship between galaxy luminosity and halo mass at infall, and determine the form of this relation by solving the implicit equation

$$n_S(>M_r) = n_H(>M_H), \tag{1}$$

where n_S and n_H are the number densities of galaxies and haloes, respectively, M_r is the galaxy r-band magnitude threshold and M_H is the halo mass threshold chosen so that the number density of haloes above it is equal to the number density of galaxies in the sample. The quantity M_H is defined as follows:

$$M_H = \begin{cases} M_{halo}(z=0) & \text{for distinct haloes,} \\ M_{halo}(z=z_{sat}) & \text{for subhaloes,} \end{cases} \tag{2}$$

where z_{sat} is the infall epoch defined as the time when a halo first enters the virial radius of a more massive halo.

2.2 GALFORM

GALFORM is a semi-analytic model of galaxy formation and evolution. In GALFORM-GP14 (Gonzalez-Perez et al. 2014), the time-scale for merging satellite galaxies with the central galaxy of its host halo due to dynamical friction is calculated according to Cole et al. (2000) and Lacey & Cole (1993). In this model, following a halo merger, each subhalo, along with the satellite galaxy it contains, is placed on a random orbit. A merger time-scale is then calculated using equation (3). The treatment of galaxy mergers in Lacey et al. (2016) is similar to Gonzalez-Perez et al. (2014), except that they replace the dynamical friction time-scale formula of Lacey & Cole (1993) with that of Jiang et al. (2008), which implicitly accounts for the effect on the dynamical friction time-scale caused by tidal stripping. The satellite galaxy is considered to have merged with its central galaxy once the merger time-scale has elapsed, provided that this happens before its host halo falls in to an even larger system, in which case a new merger time-scale is computed. In this paper, we do not make use of any of the baryonic physics implemented in GALFORM.

3 MODEL

Following halo mergers, the less massive halo continues to exist as a distinct subhalo within the more massive host halo for a period of time. Its independent existence can come to an end in one of two distinct ways. First, subhaloes can merge with the central halo after being drawn in to the centre of the host halo by dynamical friction. Secondly, subhaloes experience tidal stripping, and if sufficiently close to the centre of the host halo, they can be completely disrupted tidally. In this section, we outline how we model each of these processes.

3.1 Dynamical friction

Subhaloes in orbit within a more massive host halo experience forces from the particles of the host halo, which dissipate its energy and angular momentum, and drag it towards the centre of the host halo, where the galaxy it hosts can merge with the central galaxy of the host halo.

Starting from the calculation of acceleration from dynamical friction by Chandrasekhar (1943), Lacey & Cole (1993) derive the following expression for the merger time-scale, T_{df}, for subhaloes entering the virial radius of a more massive host halo with a singular isothermal sphere density profile.

$$T_{df} = \frac{f(\epsilon)}{2B(1)\ln\Lambda} \left(\frac{R_H}{V_c}\right) \left(\frac{r_c}{R_H}\right)^2 \left(\frac{M_H}{M_S}\right), \tag{3}$$

where $\epsilon = J/J_c$, is the ratio of the angular momentum of the actual orbit to the angular momentum of a circular orbit with the same energy, r_c is the radius of a circular orbit in the halo with the same energy as the actual orbit, R_H is the radius of the halo, $R_H/V_c = \tau_{dyn}$ is the dynamical time of the halo, M_H and M_S are the masses of the host halo and subhalo, respectively, $\ln \Lambda$ is the Coulomb logarithm taken to be $\ln(M_H/M_S)$ and

$$B(x) = \text{erf}(x) - \frac{2x\sqrt{\pi}}{\exp}(-x^2). \tag{4}$$

Although equation (3) captures the essential characteristic features of the merging of subhaloes due to dynamical friction, it makes certain simplifying assumptions. First, the density profile of dark matter haloes is assumed to be a singular isothermal sphere. While halo density profiles are approximately isothermal over a large range in radius, N-body simulations have found that they are significantly shallower than r^{-2} at small radii and steeper than r^{-2} near the virial radius (Navarro, Frenk & White 1996). Halo density profiles are better approximated by a Navarro–Frenk–White (NFW) profile given by

$$\rho(r) = \frac{\rho_0}{(r/r_s)(1 + r/r_s)^2}, \tag{5}$$

where $r_s = r_{200}/c$, r_{200} is the radius at which the average density of the halo is 200 times the critical density and c is the halo concentration parameter. Additionally, contrary to the assumptions made to carry out the above calculation, the host halo is non-spherical, its velocity dispersion is not necessarily isotropic and it is usually evolving.

Other semi-analytic models use formulae with a different dependence on the orbital parameters, different definitions of the subhalo mass or different definitions of the Coulomb logarithm. For example, Cooray & Milosavljević (2005) treat the Coulomb logarithm as a mass independent constant while others (Hashimoto et al. 2003; Zentner et al. 2005) assume that it varies with orbital parameters. Fujii, Funato & Makino (2006) argue that the bound mass does not constitute a good estimate of M_{sat} because tidally stripped material that is not formally bound to the satellite can contribute to dynamical friction. Similarly, other studies have found different dependences on angular momentum and r_c/r. For example,

van den Bosch et al. (1999) find a weaker dependence on J/J_c than Lacey & Cole (1993), while Taffoni et al. (2003) find a weaker dependence on r_c/r compared to Lacey & Cole (1993). Boylan-Kolchin et al. (2008) carried out N-body simulations of an idealized system consisting of a single subhalo in orbit around a parent halo with a Hernquist density profile, finding that an exponential dependence on circularity and a linear dependence on r_c/r provided the best fit.

In our model, following each halo merger, we track each subhalo until the point that it can no longer be resolved in the N-body simulation. We then compute the energy of the subhalo at the latest epoch that it was identified in the N-body simulation, assuming the host halo to have an NFW density profile with concentration parameter, c given by the halo mass–concentration relation. We then determine the dynamical friction time-scale, T_{df}, from equation given below:

$$T_{df} = \left(\frac{r_c}{r}\right)^{\alpha} \left(\frac{J}{J_c}\right)^{\beta} \frac{\tau_{dyn}}{2B(1)\ln\Lambda} \left(\frac{M_{int}}{M_S}\right), \tag{6}$$

where r is the orbital radius of the subhalo and M_{int} is the mass of the parent halo interior to r. In this work, we compute the mass interior to r assuming an NFW profile, but in principle it can be measured in the simulation. Note that equation (6) is similar to equation (3) of Lacey & Cole (1993), but with the terms rearranged for convenience. equation (3) is generally applied at infall i.e. when the subhalo crosses the virial radius of another halo. However, equation (6) can be applied at any point of time after infall.

Lacey & Cole (1993) set $\alpha = 2$ and $\beta = 0.78$. Their value of α comes from the analytic calculation assuming a singular isothermal sphere density profile for the host halo and their value of β was determined from numerical integration of the orbit-averaged equations for energy and angular momentum loss due to dynamical friction for a point mass in a singular isothermal sphere potential. In contrast to Lacey & Cole (1993), we treat the dependence of the dynamical friction time-scale on energy and angular momentum as free parameters. We determine both α and β numerically, finding $\alpha = 1.8$ and $\beta = 0.85$. We discuss the details of the procedure for determining these parameters in Section 4. Additionally, in Lacey & Cole (1993), r_c and J_c are calculated assuming a singular isothermal sphere density profile for the host halo, while in our model, we compute these quantities assuming a NFW density profile for the host halo.

If the parent halo merges with an even larger halo before time T_{df}, we recalculate a new dynamical friction time-scale, T_{df} for the new host halo. We assume that the subhalo retains its mass and ignore the effect of tidal stripping. We ignore interactions between two orbiting subhaloes. Such interactions rarely result in mergers because satellite subhaloes are unlikely to encounter other satellite subhaloes at low enough velocities to result in a bound interaction (Wetzel, Cohn & White 2009).

3.2 Tidal disruption

A subhalo in orbit within a more massive host halo experiences tidal forces that can strip away the outer regions, or, in some cases, entirely disrupt the subhalo. Material is stripped from satellite subhaloes when the tidal force from the host halo exceeds the self-gravity of the subhalo, and the same process under extreme circumstances leads to complete disruption of the satellite subhalo.

In our model, we disrupt a satellite subhalo if the mean density of the host halo within the radius of the satellite subhalo exceeds the density of the satellite subhalo, i.e. if the distance of the subhalo

from the centre of the host halo falls below a tidal disruption radius, R_{td}, which is defined as the radius within which the mean density of the host halo exceeds the density of the satellite subhalo.

$$R_{td} = r_{sat} \sqrt[3]{\frac{M_H(<R_{td})}{M_{sat}}}, \tag{7}$$

where R_{td} is the tidal disruption radius, r_{sat} is the radius of the satellite subhalo, $M(<R_{td})$ is the mass of the host halo enclosed within R_{td} and M_{sat} is the mass of the satellite subhalo. The mass of the host halo enclosed within R_{td} is determined assuming an NFW density profile for the host halo with concentration parameter c determined from the halo mass–concentration relation, but, alternatively, it can be measured in the simulation.

We follow the position of a subhalo as long as it exists in the N-body simulation. We then compute the position of its most bound particle at the latest epoch that the subhalo was resolved. We then follow the position of this particle and treat it as the position of the subhalo. The subhalo is removed from the population if its distance from the centre of the host halo falls below the tidal disruption radius, R_{td}.

We ignore mass-loss due to tidal stripping. In our model, tidal destruction is treated as a binary process that takes effect and removes a subhalo and the galaxy it hosts from the population only when the subhalo enters a region that is denser than its own mean density.

3.3 Distribution of orbital parameters

The top panel of Fig. 1 shows the distribution of r_c/r for all subhaloes in the MS II. r_c/r is a measure of the energy of the subhalo. Subhaloes with lower values of r_c/r are more strongly bound to the central halo than subhaloes with higher values of r_c/r. The bottom panel of Fig. 1 shows the distribution of J/J_c for the same sample. J/J_c is a measure of the circularity of the orbit. $J/J_c = 1$ corresponds to a perfectly circular orbit, while $J/J_c = 0$ corresponds to a radial orbit. The distribution of orbital parameters in our simulation is broadly similar to that of Jiang et al. (2015).

Fig. 2 shows the distribution of mass ratios, M_H/M_S, where M_H is the halo mass and M_S is the subhalo mass at infall, for all subhaloes above an infall mass threshold of 8.6×10^{10} in MS II. Nearly 90 per cent of subhaloes have less than one-fifth of the mass of the host halo at infall. The number of nearly equal mass mergers is small, and in any case, most merge with the host halo on fairly short time-scales.

3.4 Determination of model parameters

Fig. 3 compares the mean number of subhaloes as a function of halo mass between the MS and MS II simulations, two N-body simulations whose mass resolutions differ by a factor of 100. We select subhaloes that are above an infall mass threshold of $8.6 \times 10^{10} \, h^{-1} \, M_{\odot}$, which corresponds to 100 times the particle mass in MS. Although the halo mass function converges for this mass threshold (Boylan-Kolchin et al. 2009), there are substantial differences in the subhalo population between MS and MS II. The higher resolution MS II retains substantially more subhaloes at $z = 0$. Although MS can adequately resolve subhaloes with more than 100 particles at infall, subhaloes are subject to tidal stripping after infall, which reduces their mass and thus renders them unresolvable in MS at later times, including at $z = 0$. However, similar mass objects can be resolved in MS II as they contain 100 times more particles.
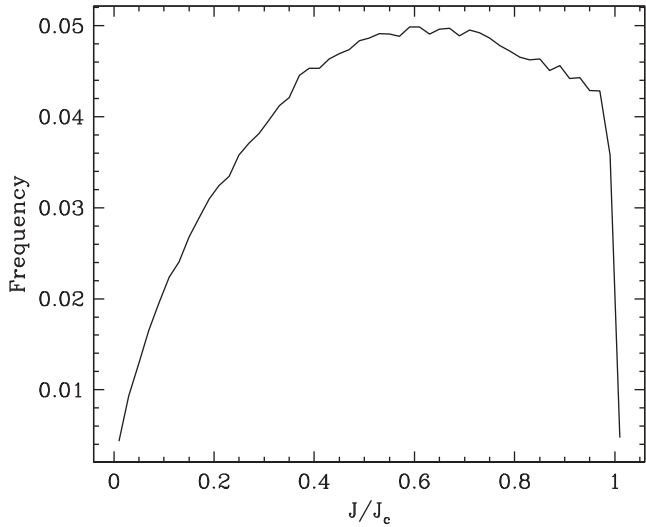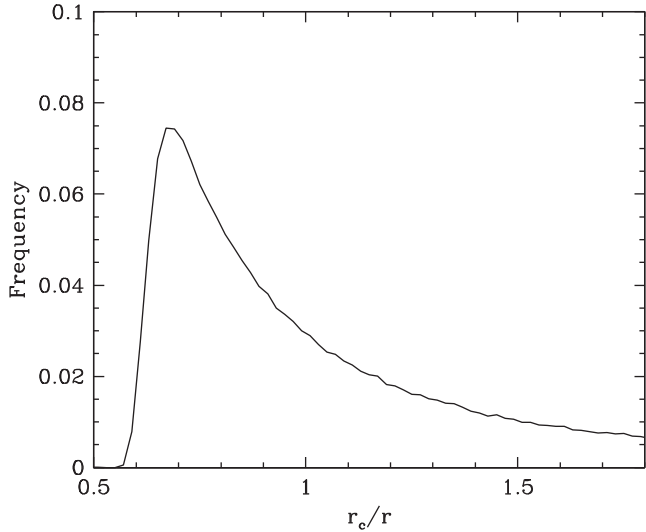
Figure 1. Top panel: the distribution of r_c/r for all subhaloes in MS II. Bottom panel: the distribution of J/J_c for all subhaloes in MS II.
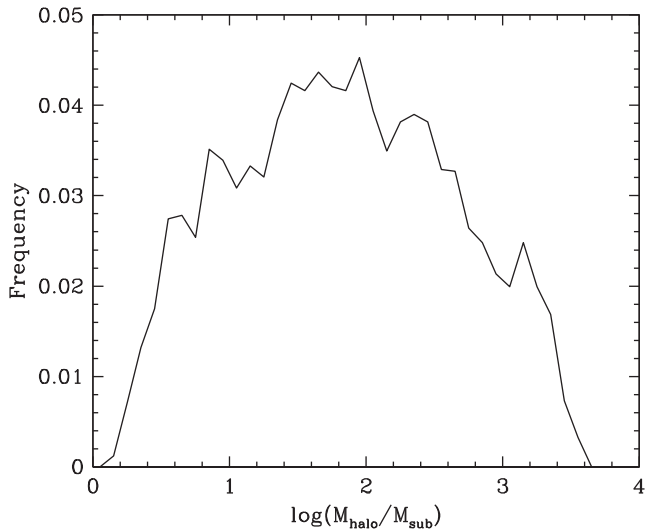

Figure 2. The distribution of mass ratios for all subhaloes above an infall mass threshold of 8.6×10^{10} in MS II.
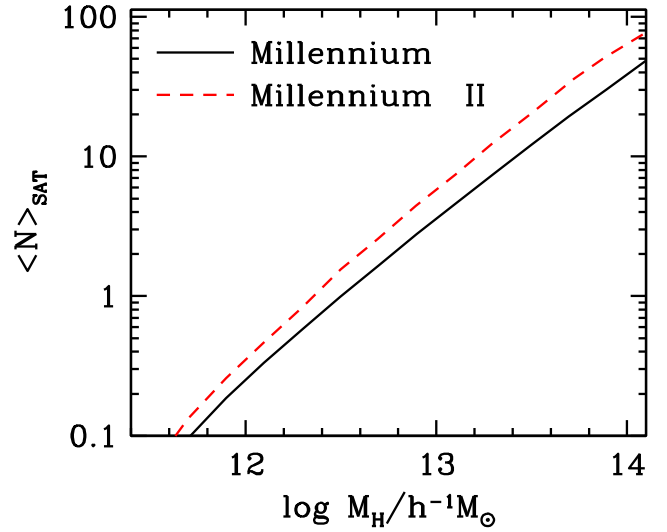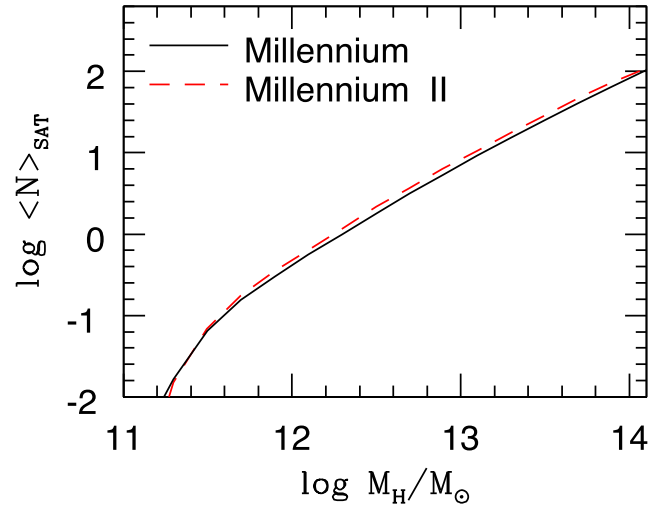

Figure 3. Mean number of subhaloes as a function of parent halo mass at $z = 0$ in MS (black solid) and MS II (red dashed). Subhaloes above an infall mass threshold of $8.6 \times 10^{10} \, h^{-1} \, \mathrm{M}_\odot$ are selected, which corresponds to 100 times the particle mass in the MS.

Figure 4. Mean number of subhaloes per halo as a function of parent halo mass at $z = 0$ after applying our model for the dynamical evolution of subhaloes. Subhaloes above an infall mass threshold of $8.6 \times 10^{10} \, h^{-1} \, \mathrm{M}_\odot$ are selected, which corresponds to 100 times the particle mass in the MS.

To track subhaloes that can no longer be resolved in the *N*-body simulation, we implement the procedure outlined in Section 3 to subhaloes in both MS and MS II. In short, subhaloes that can no longer be resolved in the *N*-body simulation are removed from the population after time T_{df}, given by equation (6), has elapsed from the last epoch the subhalo was resolved in, or if the pericentric distance between the subhalo and the centre of the host halo falls below R_{td} given by equation (7).

Fig. 4 shows the mean number of subhaloes as a function of halo mass upon applying our model to MS and MS II. Using the canonical values of $\alpha = 2$ and $\beta = 0.78$ in equation (6) produces substantially better agreement between the mean number of subhaloes as a function of host halo mass, between MS and MS II compared to Fig. 3.

However, it can be further improved by fitting our model parameters, α and β to minimize the difference in the number of subhaloes
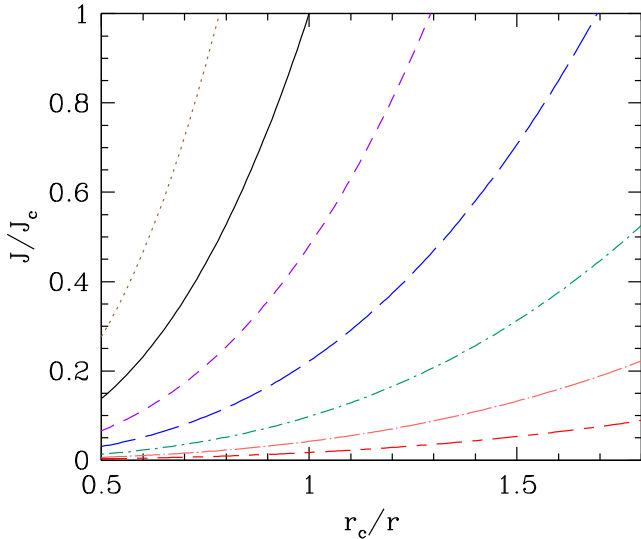
Figure 5. Dynamical friction time-scale in our model compared to GALFORM-GP14. J/J_c is plotted against r_c/r. Curves of constant $\Delta T_{df}/T_{df}$ are shown. The top most, brown dotted curve is the set of orbital parameter values for which our model predicts a 5 per cent longer dynamical friction time-scale compared to GALFORM-GP14, the black solid curve is the set of orbital parameter values for which our model predicts the same dynamical friction time-scale as GALFORM-GP14, the purple short-dashed 5 per cent shorter, the blue long-dashed 10 per cent shorter, the green dot–short dashed 15 per cent shorter, the orange dot–long dashed 20 per cent shorter and the red short dashed–long dashed 25 per cent shorter.

in bins of host halo mass between MS and MS II. We minimize the following quantity

$$\sum_i |N_{sub}(MS)_i - N_{sub}(MS\ II)_i|, \tag{8}$$

where the summation is carried out over bins of halo mass. We find that $\alpha = 1.8$ and $\beta = 0.85$ provides the best fit. For the canonical values of $\alpha = 2$ and $\beta = 0.78$, the HOD differ by 10 per cent, whereas for our best-fitting values of $\alpha = 1.8$ and $\beta = 0.85$, the HODs agree to better than 2 per cent.

We have checked that our results are not sensitive to the mass threshold used in Figs 3 and 4.

3.5 Comparison with GALFORM-GP14

Our model, presented in this paper, differs from that of GALFORM-GP14 in three ways. First, in GALFORM-GP14, subhaloes are placed on random orbits following infall. In contrast, in our model, we use the subhalo infall parameters and follow the evolution of the subhalo up to the latest epoch that it can be resolved in the simulation. Secondly, in our model, the scaling of the merger time-scale with the energy and angular momentum of the subhalo is different (compare equation 6 to equation 3). Finally, we implement a physically motivated prescription for tidal destruction of subhaloes. In this subsection, we examine the effects of each of these.

Fig. 5 shows the difference in dynamical friction time-scales between our model and GALFORM-GP14 as a function of the orbital parameters, r_c and J_c. Curves of constant $\Delta T_{df}/T_{df}$ are shown, where ΔT_{df} is the difference between the dynamical friction time-scale in our model and GALFORM-GP14. For the range of values of the orbital parameters that we obtain in our simulation, the dynamical friction time-scale we predict is between 30 per cent shorter and 10 per cent longer than GALFORM-GP14. Compared
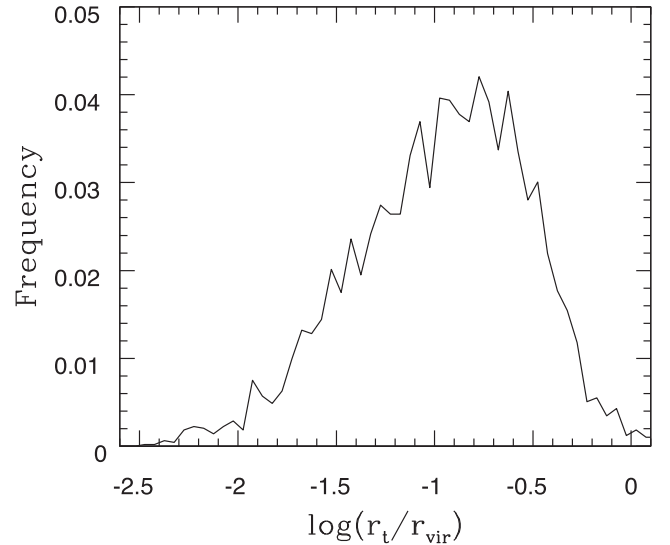

Figure 6. Histogram of the tidal radius of subhaloes in units of the parent halo virial radius, when our model is applied to MS II without our prescription for tidal destruction.

to GALFORM-GP14, we predict shorter merging time-scales for more radial orbits, and for orbits with higher energy.

Besides the values of α and β, our equation (6) uses different halo and subhalo masses compared to equation (3) used in GALFORM-GP14. We use the subhalo mass at the last epoch the subhalo was resolved in our simulation in contrast to GALFORM-GP14, which uses the subhalo mass at infall. Additionally, instead of the halo mass, M_H used in GALFORM-GP14, we use the mass interior to the orbital radius, r, M_{int}.

In GALFORM-GP14, the only way subhaloes can be removed from the population is if their angular momentum goes to zero because of dynamical friction. This results in a substantial population of subhaloes at very small distances from the centre of the parent halo. Fig. 6 shows a histogram of the tidal radii of subhaloes in units of the parent halo virial radius, when our model is applied without our prescription for tidal destruction. There is a population of subhaloes that are no longer resolved in the simulation, but have not yet merged with the central halo through dynamical friction. Of these, a significant fraction have tidal radii that are much smaller than the typical size of subhaloes. The tidal radii of many of these subhaloes are also much smaller than their own size when they were last resolved in the simulation. To combat this problem, we implement a physically motivated prescription for tidal destruction that removes a subhalo from the population if its mean density is less than the mean density of the host halo interior to its orbital radius.

4 RESULTS

In this section, we investigate the implications of our model for the dynamical evolution of subhaloes for studies of galaxy clustering. One plausible method of comparing our model to the raw *N*-body simulation would be to apply identical baryonic physics to the raw *N*-body merger trees and those derived by applying our model to the *N*-body merger trees. However, such an approach would produce galaxy catalogues with different galaxy stellar mass functions. An alternative approach is to tune the baryonic physics independently in each case to match certain observables like the galaxy stellar mass function. However, that would still leave us with the difficulty of disentangling differences due to different baryonic physics from
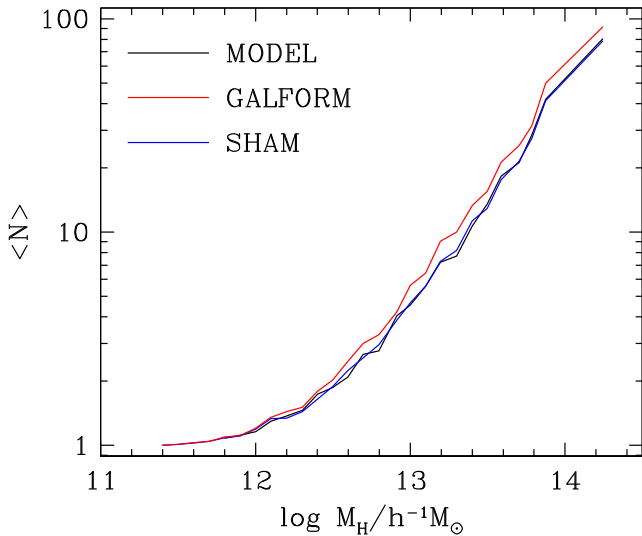
Figure 7. Halo occupation distribution of the model presented in this paper compared with two other models. GALFORM-GP14 is based on Gonzalez-Perez et al. (2014) and SHAM is abundance matching on the raw *N*-body simulation.
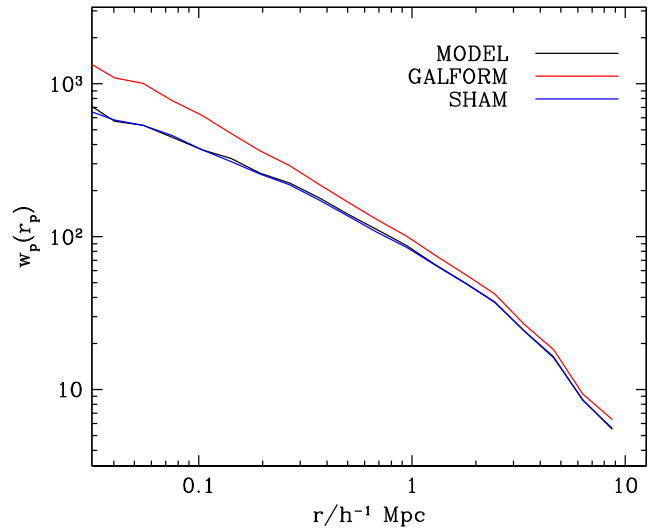

Figure 8. Projected two-point correlation function of galaxies in the model presented in this paper compared with two other models. GALFORM-GP14 is based on Gonzalez-Perez et al. (2014) and SHAM is abundance matching on the raw *N*-body simulation.

the differences due to the treatment of the dynamic evolution of subhaloes.

In this paper, instead of explicit assumptions about the baryonic physics, we employ SHAM to construct our galaxy catalogues. We compare our model for the dynamical evolution of subhaloes with two other models for the dynamical evolution of subhaloes, which produce different populations of surviving subhaloes. First, SHAM carried out on the raw *N*-body simulation where we consider only subhaloes that survive until $z = 0$ in the *N*-body simulation. Secondly, the method used by GALFORM-GP14 for evolving subhaloes and satellite galaxies discussed in Section 2.2. We do not make use of any of the baryonic physics implemented in GAL-FORM. Our model and GALFORM-GP14 are applied to the MS, while for the raw *N*-body simulation, we use the higher resolution MS II.

In all three cases, we populate our subhaloes with galaxies using SHAM. The number density of objects is $3.03 \times 10^{-2} \, h^3 \, \mathrm{Mpc}^3$, which corresponds to the number density of objects brighter than M_r of -18 in SDSS DR7 (Zehavi et al. 2011). In all three cases, the number density of galaxies and the galaxy luminosity functions are identical. The differences between the catalogues arise solely from the different treatments of subhaloes following halo mergers, which manifest themselves as differences in the satellite galaxy fractions, which, in turn, affect HODs and clustering statistics.

Fig. 7 compares the $z = 0$ halo occupation distribution of our model to that obtained from abundance matching on the raw *N*-body merger trees and GALFORM-GP14's treatment of the evolution of subhaloes. At the resolution of Fig. 7, where subhaloes have $\approx 2 \times 10^4$ particles, the differences between our model and the raw *N*-body merger trees are small, although our model will recover a similar halo occupation distribution even with a lower resolution *N*-body simulation. However, the GALFORM-GP14 model retains significantly more subhaloes than either of the other two models. Note that all models are constrained to have the same number of galaxies, but each model has a different number of central and satellite galaxies. While the satellite fractions of our model and SHAM on the raw *N*-body merger tree are within 1 per cent of

each other, the satellite fraction in the GALFORM-GP14 model is 19 per cent higher.

Fig. 8 compares the $z = 0$ projected two-point correlation function of galaxies in our model to that obtained from abundance matching on the raw *N*-body merger trees and GALFORM-GP14's treatment of the evolution of subhaloes, and Fig. 9 shows the ratio of the correlation function produced by abundance matching on the raw *N*-body merger trees and GALFORM-GP14's treatment of the evolution of subhaloes and our model. On scales below $\approx 1 \, h^{-1}$ Mpc, the galaxy two-point correlation function is determined by pairs of objects within haloes – the 'one-halo term'. Since the GALFORM-GP14 model contains 19 per cent more satellite galaxies, it produces a higher clustering amplitude that can be up to twice as high as the clustering amplitude in our model on certain scales. The clustering of galaxies in our model and abundance matching on the raw *N*-body merger trees agree to better than 5 per cent, reflecting the fact that they contain a similar fraction of subhaloes.

On scales larger than $\approx 1 \, h^{-1}$ Mpc, the two-point correlation function is determined by pairs of galaxies in different haloes known as the 'two-halo term'. Since the overall number density of objects and the positions of haloes are the same in all models, there are only small differences on these scales.

5 DISCUSSION AND CONCLUSIONS

We present a model for the dynamical evolution of subhaloes based on an approach that combines numerical and analytical methods. Our method is based on tracking subhaloes in an *N*-body simulation up to the point that it can be resolved, and applying an analytic prescription for its subsequent merger time-scale that takes dynamical friction and tidal disruption into account. When applied to cosmological *N*-body simulations with mass resolutions that differ by two orders of magnitude, the technique presented in this paper produces HODs that agree to within 3 per cent.

Modelling galaxy mergers within dark matter haloes is an important ingredient of galaxy formation models. Precise estimates of galaxy merger time-scales are required for modelling galaxy
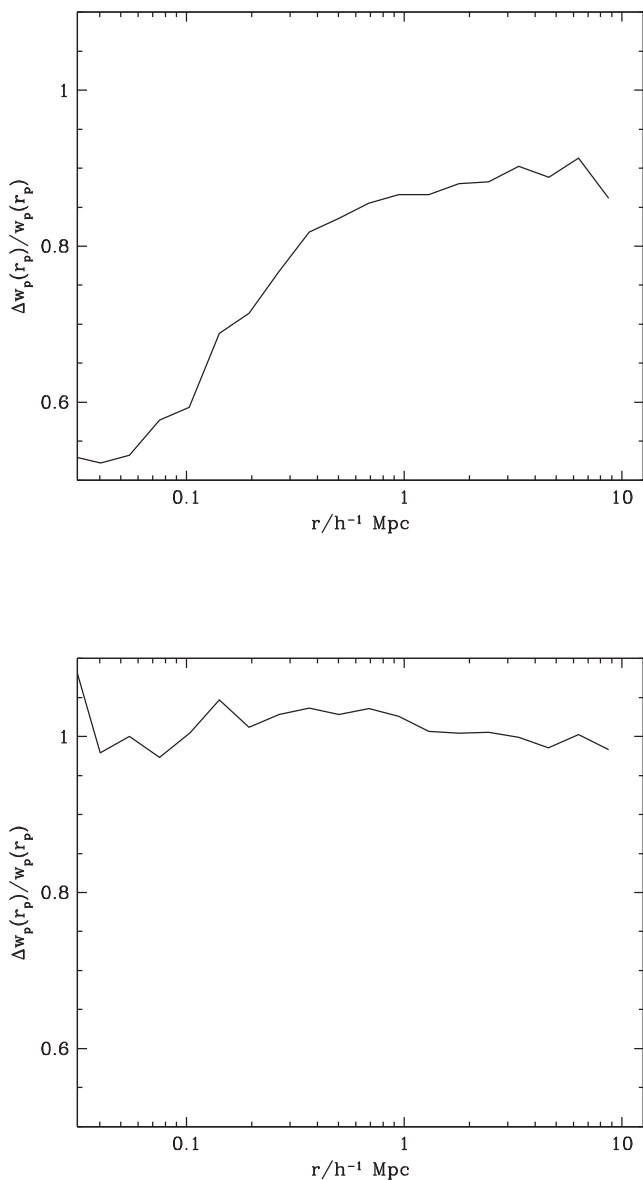
matched to observationally inferred stellar masses and find that it produces better agreement with the observed small-scale clustering in SDSS at $z = 0.1$ and GAMA at $z = 0.2$ (see figs 7 and 8 of Campbell et al. 2015). McCullagh et al. (in preparation) apply our model to an *N*-body simulation that is similar to the MS, but with cosmological parameters determined by the *Planck* mission (Planck Collaboration XIII 2015). They examine the HODs and galaxy clustering and find better agreement with data from SDSS compared to GALFORM-GP14.

Our results are based on examining dark matter only simulations. Our model does not include the effect of baryons. Although stellar mass typically constitutes less than 10 per cent of the halo virial mass, baryons are more strongly concentrated than dark matter and more dense than dark matter at a given scale. As a result, they are more resistant to disruption. While including baryons reduces the likelihood of tidal disruption, it shortens the dynamical friction time-scale. By comparing simulations with and without stellar bulges, Boylan-Kolchin et al. (2009) find that the effect of baryons on merger time-scales is typically less than 10 per cent. To shed further light on these issues, we plan to compare our prescription with hydrodynamic cosmological simulations in future work.

We emphasize that the model presented in this paper for the dynamical evolution of subhaloes uses the information in an *N*-body simulation, but can produce results that are not affected by artificial disruption of subhaloes due to limited resolution.

ACKNOWLEDGEMENTS

Figure 9. Top panel: ratio of the projected two-point correlation function of galaxies in GALFORM-GP14 Gonzalez-Perez et al. (2014) and the model presented in this paper. Bottom panel: ratio of the projected two-point correlation function of galaxies from abundance matching on the raw *N*-body simulation and the model presented in this paper.

clustering, mass assembly of galaxies, properties of satellite galaxies and black hole merger rates.

While subhaloes that approach the host halo too closely can be tidally destroyed in our model, we do not model mass-loss due to tidal stripping and its effects on the dynamical friction time-scale. We also ignore satellite–satellite interactions, which, in any case, are rare.

Our model can be applied to generate mock galaxy catalogues from *N*-body simulations. Furthermore, it can also be applied to build mock galaxy catalogues from Monte Carlo or other kinds of merger trees by drawing the energy and angular momentum of each subhalo from distributions similar to Fig. 1, and then applying equation (6) to determine the merger time-scale.

Campbell et al. (2015) apply our model for subhalo evolution to the GALFORM semi-analytic model with galaxy stellar masses

REFERENCES

Berlind A. A. et al., 2003, ApJ, 593, 1
Boylan-Kolchin M., Ma C.-P., Quataert E., 2008, MNRAS, 383, 93
Boylan-Kolchin M., Springel V., White S. D. M., Jenkins A., Lemson G., 2009, MNRAS, 398, 1150
Campbell D. J. R. et al., 2015, MNRAS, 452, 852
Chandrasekhar S., 1943, ApJ, 97, 255
Cole S., Lacey C. G., Baugh C. M., Frenk C. S., 2000, MNRAS, 319, 168
Colín P., Klypin A. A., Kravtsov A. V., Khokhlov A. M., 1999, ApJ, 523, 32
Conroy C., Wechsler R. H., Kravtsov A. V., 2006, ApJ, 647, 201
Cooray A., Milosavljević M., 2005, ApJ, 627, L85
Davis M., Efstathiou G., Frenk C. S., White S. D. M., 1985, ApJ, 292, 371
Fujii M., Funato Y., Makino J., 2006, PASJ, 58, 743
Gonzalez-Perez V., Lacey C. G., Baugh C. M., Lagos C. D. P., Helly J., Campbell D. J. R., Mitchell P. D., 2014, MNRAS, 439, 264
Hashimoto Y., Funato Y., Makino J., 2003, ApJ, 582, 196
Jiang C. Y., Jing Y. P., Faltenbacher A., Lin W. P., Li C., 2008, ApJ, 675, 1095
Jiang L., Cole S., Sawala T., Frenk C. S., 2015, MNRAS, 448, 1674
Kazantzidis S., Mayer L., Mastropietro C., Diemand J., Stadel J., Moore B., 2004, ApJ, 608, 663

Klypin A., Kravtsov A. V., Valenzuela O., Prada F., 1999, ApJ, 522, 82
Kravtsov A. V., Berlind A. A., Wechsler R. H., Klypin A. A., Gottlöber S., Allgood B., Primack J. R., 2004, ApJ, 609, 35
Lacey C., Cole S., 1993, MNRAS, 262, 627
Lacey C. G. et al., 2016, MNRAS, 462, 3854
Moore B., Quinn T., Governato F., Stadel J., Lake G., 1999, MNRAS, 310, 1147
Moster B. P., Somerville R. S., Maulbetsch C., van den Bosch F. C., Macciò A. V., Naab T., Oser L., 2010, ApJ, 710, 903
Nagai D., Kravtsov A. V., 2005, ApJ, 618, 557
Navarro J. F., Frenk C. S., White S. D. M., 1996, ApJ, 462, 563
Planck Collaboration XIII, 2015, A&A, 594, A13
Saro A., De Lucia G., Dolag K., Borgani S., 2008, MNRAS, 391, 565
Simha V., Weinberg D. H., Davé R., Fardal M., Katz N., Oppenheimer B. D., 2012, MNRAS, 423, 3458
Spergel D. N. et al., 2003, ApJS, 148, 175
Springel V., White S. D. M., Tormen G., Kauffmann G., 2001, MNRAS, 328, 726
Springel V. et al., 2005, Nature, 435, 629

Stewart K. R., Bullock J. S., Barton E. J., Wechsler R. H., 2009, ApJ, 702, 1005
Taffoni G., Mayer L., Colpi M., Governato F., 2003, MNRAS, 341, 434
Trujillo-Gomez S., Klypin A., Primack J., Romanowsky A. J., 2011, ApJ, 742, 16
Vale A., Ostriker J. P., 2004, MNRAS, 353, 189
Vale A., Ostriker J. P., 2006, MNRAS, 371, 1173
van den Bosch F. C., Lewis G. F., Lake G., Stadel J., 1999, ApJ, 515, 50
van den Bosch F. C. et al., 2007, MNRAS, 376, 841
Wetzel A. R., Cohn J. D., White M., 2009, MNRAS, 395, 1376
Zehavi I. et al., 2011, ApJ, 736, 59
Zentner A. R., Berlind A. A., Bullock J. S., Kravtsov A. V., Wechsler R. H., 2005, ApJ, 624, 505
Zheng Z. et al., 2005, ApJ, 633, 791

This paper has been typeset from a TeX/LaTeX file prepared by the author.